Korean J. Chem. Eng., 34(1), 214-224 (2017)
DOI: 10.1007/s11814-016-0233-0

pISSN: 0256-1115
eISSN: 1975-7220

Density, refractive index and kinematic viscosity of MIPK, MEK and phosphonium-based ionic liquids and the excess and deviation properties of their binary systems

Kyeong-Ho Lee*, So-Jin Park*,†, and Young-Yoon Choi**

*Department of Chemical Engineering, College of Engineering, Chungnam National University, Daejeon 34134, Korea
**Minerals and Materials Processing Division, Korea Institute of Geoscience and Mineral Resources, Daejeon 34132, Korea
(*Received 2 June 2016 • accepted 11 August 2016*)

Abstract−The density, refractive index, and kinematic viscosity were measured for extraction solvents for molybdenum: methyl ethyl ketone (MEK), methyl isopropyl ketone (MIPK), trihexyl tetradecyl phosphonium chloride ([$P_{666,14}$][Cl]), trihexyl tetradecyl phosphonium dicyanamide ([$P_{666,14}$][DCA]) and trihexyl tetradecyl phosphonium bis (2,2,4-trimethyl pentyl) phosphinate ([$P_{666,14}$][TMPP]) at atmospheric pressure for a temperature range of 288.15-318.15 K. The experimental data were correlated using the Daubert and Danner equation, a linear equation and the Goletz and Tassion equation. In addition, the excess molar volumes (V^E) and the deviations in molar refractivity (ΔR) at 298.15 K were reported for the following binary systems: {MEK+[$P_{666,14}$][Cl]}, {MEK+[$P_{666,14}$][DCA]}, {MEK+[$P_{666,14}$][TMPP]}, {MIPK+[$P_{666,14}$][Cl]}, {MIPK+[$P_{666,14}$][DCA]} and {MIPK+[$P_{666,14}$][TMPP]}. The determined V^E and ΔR values were correlated with the Redlich-Kister equation. The binary density and refractive index data at 298.15 K were also predicted using several mixing rules, and these results were then compared with the experimental data.

Keywords: Density, Refractive Index, Kinetic Viscosity, Excess Property, Deviation Property

INTRODUCTION

Molybdenum (Mo) is a high-melting metal that is used in small quantities to harden steel, and it is therefore used in many alloys. It is typically extracted using amine or ketone type organic solvents, such as trioctyl amine (TOA) or an acetyl acetone from an acid leached Mo solution. In previous work, we reported that some organics and ionic liquids--methyl isopropyl ketone (MIPK), methyl ethyl ketone (MEK), trihexyl tetradecyl phosphonium chloride ([$P_{666,14}$][Cl]), trihexyl tetradecyl phosphonium dicyanamide ([$P_{666,14}$][DCA]) and trihexyl tetradecyl phosphonium bis(2,2,4-trimethylpentyl) phosphinate ([$P_{666,14}$][TMPP])--can be used as effective solvents and diluents in the Mo extraction process [1].

In this work, we studied the density (ρ), refractive index (n_D) and kinematic viscosity (ν) for MIPK, MEK and the aforementioned phosphonium-based ionic liquids under atmospheric pressure at a range of temperatures from 288.15 to 318.15 K. In addition, the excess and deviation properties from the ideal conditions for the excess molar volumes (V^E) and the deviations of the refractive indices (ΔR) were determined at 298.15 K over the entire composition ranges for the following binary mixtures: {MEK+[$P_{666,14}$][Cl]}, {MEK+[$P_{666,14}$][DCA]}, {MEK+[$P_{666,14}$][TMPP]}, {MIPK+[$P_{666,14}$][Cl]}, {MIPK+[$P_{666,14}$][DCA]} and {MIPK+[$P_{666,14}$][TMPP]}. These mixtures were chosen because they are very essential in the cosolvent design of the Mo extraction and solvent recycling processes. And for the relative ease in characterizing the type and magnitude of molecular interactions upon mixing for evaluation of thermodynamic model parameters, especially for the substances such as ionic liquids [2,3].

The experimental excess and deviation properties were satisfactorily correlated with the Redlich-Kister polynomial [4]. In contrast, the Lorentz-Lorenz [5], Gladstone-Dale [6], Weiner [7] and Heller [8] mixing rules were applied to predict the refractive index of mixtures, while the density of the mixture was estimated using an expression based on the Lorentz-Lorenz mixing rule [2]. These predicted density and refractive indices were subsequently compared with the experimental data.

EXPERIMENTAL SECTION

1. Materials

All chemicals were supplied by Sigma Aldrich (USA). The mass purities of MEK and MIPK were greater than 99.9% by G.C. analysis, while the mass purities of [$P_{666,14}$][Cl], [$P_{666,14}$][DCA], and [$P_{666,14}$][TMPP] were better than 95.0%, according to the suppliers. All chemicals were dried using molecular sieves with a pore diameter of 0.3 nm. The water content of the MEK and MIPK, determined using a Karl-Fischer titrator (Metrohm 684 KF-Coulometer), was less than 2×10^{-5} g·g^{-1}, and that of the ionic liquids was less than 7×10^{-4} g·g^{-1}. The thermo-physical properties and purities of the chemicals are summarized in Table 1, along with the reported literature values [9-13].

2. Apparatus and Procedure

The density (ρ) measurements were conducted at atmospheric pressure, based on the vibrating tube measuring method. The DMA 5000 (Anton Paar) densitometer was utilized for these experiments.

†To whom correspondence should be addressed.
E-mail: sjpark@cnu.ac.kr

Table 1. Purity and physical properties of the chemicals utilized in this study at T=298.15 K and *p*=0.1 MPa

Chemicals	Source	Purification method	GC analysis (wt%)	ρ/g·cm^{-3} [a]		n_D [b]	
				Expt.	Lit.	Expt.	Lit.
MEK	Sigma Aldrich	Drying by molecular sieve	>99.9	0.79979	0.79989[9]	1.37641	1.3764[10]
MIPK	Sigma Aldrich	Drying by molecular sieve	>99.9	0.79882	0.79955[11]	1.38598	1.38620[11]
$[P_{666,14}][Cl]$	Sigma Aldrich	Drying by molecular sieve	-	0.88947	0.89182[12]	1.48156	1.48175[12]
$[P_{666,14}][DCA]$	Sigma Aldrich	Drying by molecular sieve	-	0.89991	0.89950[13]	1.48250	-
$[P_{666,14}][TMPP]$	Sigma Aldrich	Drying by molecular sieve	-	0.88535	0.88643[12]	1.47132	1.47125[12]

[a]Standard uncertainties u are $u(\rho)=6\times10^{-5}$ g·cm^{-3}, u(T)=0.01 K
[b]Standard uncertainties u are $u(n_D)=1.5\times10^{-4}$, u(T)=0.05 K

Long-term drift was automatically eliminated by a reference oscillator built into the measuring cell, and only one adjustment at 293.15 K was sufficient to reach a high accuracy density measurement for the whole temperature range. The DMA 5000 allows for a full-range viscosity correction, whereby all of the viscosity related errors inherent to all of the known types of the oscillating U-tube density meters were automatically eliminated. The temperature of the U-tube was controlled within 0.001 K and measured by a high-precision platinum resistance probe with an accuracy of 0.01 K. Therefore, the accuracy of the temperature was estimated at 0.01 K. For the densitometer calibration, standard water and air were used. The experimental procedure has been described in detail elsewhere [14].

The refractive indexes (n_D) of the pure components and mixtures were measured using a digital precision refractometer (KEM, model RA-520N, Kyoto, Japan). The experimental procedure has been described in detail elsewhere [15]. Approximately 3 ml of the pure and mixture samples was prepared in a ca. 5-ml vials using a microbalance (OHAUS Co. DV215CD) with a precision of 1×10^{-5} g. For the mixtures, the heavier component was added first to minimize vaporization. The sample mixtures were simultaneously prepared for the density and refractive index measurements to avoid significant experimental error due to evaporated mass. The experimental systematic error was estimated to be less than 1×10^{-4} in the mole fraction. The time interval for recording the measurements was chosen to be 15 min to attain a constant temperature via sufficient heat transfer as well as for a stable condition of the measurement.

The viscosity (η) was determined from the directly measured kinematic viscosities (ν) using an Ubbelohde viscometer with an automatic measuring unit (LAUDA, model PVS1, Germany) and a precision thermostat with a standard uncertainty of 0.01 K. The accuracy of the flowing time measurement was 0.01 s. The samples were transferred to the viscometer cell and kept there for more than 30 min to reach the desired temperature in the thermostat. And then, the sample was pumped up through the capillary of the viscometer until the upper part of the measuring cell was filled with the fixed volume of the sample (approximately 12 cm^3). Thereafter, the sample flowed down through the capillary, whereby the required flowing time was carefully recorded. Every sample was analyzed three times automatically, and the mean flowing time value was calculated. The measurement range of the Ubbelohde viscometer utilized in this experiment was 0.5 to 3,000 mm^2·s^{-1} [16].

RESULTS AND DISCUSSION

1. Pure Compound Properties

The measured densities, refractive indices and kinematic viscosities for pure components are listed in Tables 2 through 4. The standard uncertainty of the measurement for these properties, $u(X_i)$ was calculated from Eq. (1) with the largest standard deviation among the measured temperature ranges and components.

$$u(X_i)=\sqrt{\frac{\Sigma_i^N(X_i-\overline{X})^2}{N(N-1)}} \quad (1)$$

where X_i is the experimental property data of the component i, $\overline{X}$ is the mean of multiple experimental data points, and N is the number of experimental data points. The standard uncertainty reported

Table 2. Experimental densities at *p*=0.1 MPa

T/K	ρ/g·cm^{-3} [a]				
	MEK	MIPK	$[P_{666,14}][Cl]$	$[P_{666,14}][DCA]$	$[P_{666,14}][TMPP]$
288.15	0.81023	0.80859	0.89568	0.90581	0.89172
293.15	0.80502	0.80376	0.89260	0.90287	0.88848
298.15	0.79979	0.79882	0.88947	0.89991	0.88535
303.15	0.79454	0.79379	0.88630	0.89770	0.88235
308.15	0.78925	0.78880	0.88321	0.89409	0.87936
313.15	0.78393	0.78383	0.88024	0.89123	0.87639
318.15	0.77858	0.77879	0.87728	0.88836	0.87342

[a]Standard uncertainties u are $u(\rho)=6\times10^{-5}$ g·cm^{-3} and standard uncertainty u is u(T)=0.01 K

Table 3. Experimental refractive index data at p=0.1 MPa

T/K	n_D[a]				
	MEK	MIPK	$[P_{666,14}][Cl]$	$[P_{666,14}][DCA]$	$[P_{666,14}][TMPP]$
288.15	1.38135	1.39076	1.48501	1.48582	1.47433
293.15	1.37888	1.38850	1.48326	1.48412	1.47286
298.15	1.37641	1.38598	1.48156	1.48249	1.47132
303.15	1.37384	1.38322	1.47983	1.48080	1.46971
308.15	1.37101	1.38074	1.47807	1.47919	1.46809
313.15	1.36831	1.37823	1.47639	1.47756	1.46644
318.15	1.36599	1.37556	1.47467	1.47593	1.46479

[a]Standard uncertainties u are $u(n_D)=1.5\times10^{-4}$ and standard uncertainty u is u(T)=0.05 K

in this work is absolute standard uncertainty and quite referring to the degree of repeatability, and the probability in this range was roughly 68%. That is 0.68 level of confidence.

By the way, recently Laesecke et al. [17] and Fortin et al. [18] reported more realistic combined standard uncertainty for density (ρ) measurement. The averaged combined standard uncertainty ($u(\rho)$) for N density measurements can be expressed as:

$$u(\rho)=\sqrt{\frac{1}{N}S_\rho^2+u_\gamma^2+u_i^2+u_T^2} \quad (2)$$

where S_ρ, u_γ, u_i, u_T are uncertainty due to the standard deviation of the average, resolution of the instrument, instrument's varied response with density range, and the contribution due to the uncertainty in measured temperature, respectively. The calculated S_ρ was 0.000058 g·cm^{-3}, u_γ was 0.000005 g·cm^{-3}, u_i was 0.00004 g·cm^{-3} and u_T was 0.00001 g·cm^{-3} in this work. Therefore, the averaged combined standard uncertainty was calculated less than $u(\rho)=6\times10^{-5}$ g·cm^{-3} from Eq. (2). However, the impurity of sample makes the standard uncertainty much larger according to Chirico et al. [19]. Therefore, when accounting the impurity of ionic liquids, their standard uncertainty of measured density in this work would be larger than 6×10^{-5} g·cm^{-3}.

For the case of refractive indices (n_D), the standard uncertainty of the refractive indices ($u(n_D)$) was estimated less than 1.5×10^{-4} according to Eq. (1). And for kinematic viscosity (ν), standard deviation was calculated by multiplying viscometer constant to efflux time as experimental property. Every viscometer has different measuring ranges and also different viscometer constant. Therefore, we calculated individual standard deviation for each chemical, because there are quite different viscosity ranges according to the chemicals and temperatures. The averaged value of standard uncertainty, $\bar{u}(\nu)$, according to measured temperatures was calculated for each chemical as follows:

$\bar{u}(\nu)$=0.001 mm^2 s^{-1} (cSt) for MEK and MIPK,
$\bar{u}(\nu)$=0.64 mm^2 s^{-1} (cSt) for $[P_{666,14}][Cl]$,
$\bar{u}(\nu)$=0.06 mm^2 s^{-1} (cSt) for $[P_{666,14}][DCA]$,
$\bar{u}(\nu)$=0.46 mm^2 s^{-1} (cSt) for $[P_{666,14}][TMPP]$

As mentioned, the standard uncertainty, $u(\nu)$, which was represented using footnotes in Table 4, is the calculated value that with the largest standard deviation for each of chemicals. Meanwhile, according to the Widegren et al. [20], viscosities of ionic liquids are strongly influenced by contained water as impurity. According to their experiment, 700 ppm water in hydrophobic ionic liquid can decrease viscosity more than 2% of determined viscosity. The ionic liquid used here had water less than 700 ppm, and it was increased for about 80 ppm during the viscosity determination. Therefore, even though there is no reported water dependence to viscosity for the ionic liquid used this work, dissolved water may exert some influence to the determined viscosity. However, we did not consider this effect for estimating standard uncertainty in the viscosity measurement.

Table 4. Experimental kinematic viscosity data at p=0.1 MPa

T/K	ν/mm^2·s^{-1}[a]				
	MEK	MIPK	$[P_{666,14}][Cl]$	$[P_{666,14}][DCA]$	$[P_{666,14}][TMPP]$
288.15	0.500	0.607	-	573.201	1223.349
293.15	-	0.579	2887.929	421.839	853.341
298.15	-	0.555	1874.910	317.931	603.540
303.15	-	0.527	1356.951	231.359	456.159
308.15	-	0.503	950.541	179.335	341.130
313.15	-	-	687.930	143.880	251.017
318.15	-	-	499.470	114.357	193.929

[a]Standard uncertainties u are $u(\nu)$=0.001 mm^2·s^{-1} for MEK and MIPK, $u(\nu)$=1.25 mm^2·s^{-1} for $[P_{666,14}][Cl]$, $u(\nu)$=0.13 mm^2·s^{-1} for $[P_{666,14}][DCA]$, $u(\nu)$=0.89 mm^2·s^{-1} for $[P_{666,14}][TMPP]$ and standard uncertainty u is u(T)=0.01 K. The range of the Ubbelohde viscometer utilized in this experiment was 0.5 to 3,000 mm^2·s^{-1}

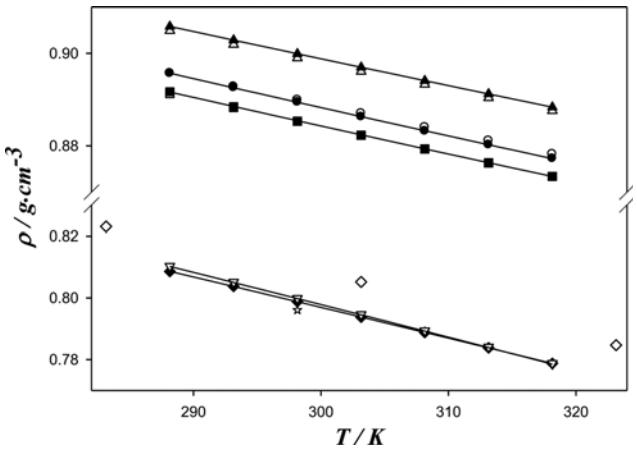

Fig. 1. Density vs temperature at p=0.1 MPa. ▼, MEK; ◆, MIPK; ●, [$P_{666,14}$][Cl]; ▲, [$P_{666,14}$][DCA]; ■, [$P_{666,14}$][TMPP]; ▽, MEK was reported by Faranda et al. [9]; ◇, MIPK was reported by Rintelen et al. [22]; ☆, MIPK was reported by Fermeglia et al. [23]; ○, [$P_{666,14}$][Cl]; △, [$P_{666,14}$][DCA]; □, [$P_{666,14}$][TMPP] were reported by Neves et al. [21]. Solid lines were calculated using the DIPPR model parameters.

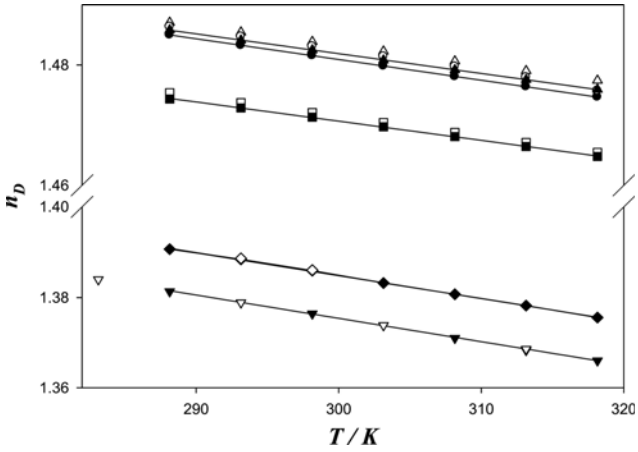

Fig. 2. Refractive indicies vs temperature at p=0.1 MPa. ▼, MEK; ◆, MIPK; ●, [$P_{666,14}$][Cl]; ▲, [$P_{666,14}$][DCA]; ■, [$P_{666,14}$][TMPP]; ▽, MEK was reported by by Clará et al. [24]; ◇, MIPK was reported by Mears et al. [25]; ☆, MIPK was reported by Fermeglia et al. [23]; ○, [$P_{666,14}$][Cl]; △, [$P_{666,14}$][DCA]; □, [$P_{666,14}$][TMPP] were reported by Almeida et al. [26]. Solid lines were calculated using the linear equation parameters.

Figs. 1 through 3 illustrate experimental pure physical properties with recalculated values (solid lines) from each model equation and with those of reported data [9,21-26]. The DIPPR (Daubert and Danner) model [27,28] was used for fitting the measured densities. It can be expressed as

$$\rho/\mathrm{g\cdot cm^{-3}} = a/[b^{1+\{1-(T/K)/c\}^d}] \quad (3)$$

where a, b, c and d are adjustable parameters. For the regression of parameters, we calculated many times according to the different initial values, and took the parameters that gave a minimum standard deviation. The correlated parameters are listed in Table 5 with their corresponding standard deviations.

The standard deviation of the fit, σ_{st}, is defined as

$$\sigma_{st} = \sqrt{\frac{\Sigma_i^N (X_i^{calc} - X_i^{exp})^2}{(N-n)}} \quad (4)$$

where X_i^{calc} and X_i^{exp} are the calculated and experimental property of the component i, respectively. N is the number of experimental data points, and n is the number of fitted parameters. As reported in Table 5, for all of the tested compounds, the σ_{st} values by the DIPPR model were less than 2.2×10^{-4}.

The experimental data were also compared with reported data. As shown in Fig. 1, the comparison of density with the literature values agreed well with mean deviations of 0.03% for MEK [9] and 0.1% for [$P_{666,14}$][Cl] and [$P_{666,14}$][DCA] and 0.01% for [$P_{666,14}$][TMPP] [21]. While MIPK showed relatively large deviation with 1.4% at 303.15 K with that of Rintelen et al. [22]; however, the other data of Fermeglia et al. [23] agreed well within 0.35% deviation.

The experimental refractive indices for pure components were fitted with a linear equation [27]:

$$n_D = I + S\cdot(T/K) \quad (5)$$

where I and S are adjustable parameters. These parameters and calculated standard deviations for n_D are reported in Table 6. A

Table 5. Parameters and standard deviations for the densities calculated using the DIPPR model

	MEK	MIPK	[$P_{666,14}$][Cl]	[$P_{666,14}$][DCA]	[$P_{666,14}$][TMPP]
a	0.0964	0.0471	0.5809	0.5751	0.5601
b	0.2995	0.2105	0.7167	0.7182	0.7081
c	543.07	600.88	461.19	512.18	496.08
d	0.3527	0.2947	1.2286	1.1947	1.2173
σ_{st}	3.0×10^{-5}	5.0×10^{-5}	5.9×10^{-5}	1.3×10^{-5}	8.2×10^{-5}

Table 6. Parameters and standard deviations for the refractive indices calculated using linear equation

	MEK	MIPK	[$P_{666,14}$][Cl]	[$P_{666,14}$][DCA]	[$P_{666,14}$][TMPP]
S	−5.17	−5.10	−3.45	−3.29	−3.19
I	1.5306	1.5378	1.5843	1.5806	1.5664
σ_{st}	2.7×10^{-4}	1.6×10^{-4}	1.4×10^{-4}	3.7×10^{-5}	9.3×10^{-5}

linear relation satisfactorily fit the experimental refractive index as a function of temperature. For all of the analyzed compounds, the σ_{st} values between the calculated and determined refractive indices were less than 2.7×10^{-4}. The refractive indices were also compared with the reported data as shown in Fig. 2. They agreed very well and the mean deviations of comparison were 0.02% for MEK [24], 0.01% for MIPK [25], 0.1% for [$P_{666,14}$][Cl] and [$P_{666,14}$][DCA], 0.07% for [$P_{666,14}$][TMPP] [26], respectively.

In the case of kinematic viscosities, the following Goletz and Tassion equation [27,29] was used to fit the experimental data:

$$\nu/\mathrm{mm^2 s^{-1}} = \mathrm{Ae}^{[B/\{(T/K)+C\}]} \quad (6)$$

where A, B and C are adjustable parameters. The correlated parameters of the Goletz and Tassion equation are given in Table 7. The experimental kinematic viscosities were relatively correlated well with Goletz and Tassion equation within ca. 1% mean deviations as shown in Fig. 3. Some kinematic viscosities of MEK, MIPK and [$P_{666,14}$][Cl] in this work were too high or too low. Therefore, they are missing in Table 4 because they were beyond the measuring ranges of our Ubbelohde viscometer. The experimented viscosities of MIPK and ionic liquids were also compared with reported data. As shown in Fig. 3, experimental kinematic viscosity for MIPK agreed well with that of Fermeglia et al. [23]. However, [P666,14][Cl] and [P666,14][TMPP] showed very large deviations about 35% from that of Neves et al. [21]. These large deviations may be caused mainly from the difference of the purity of samples and water content, because viscosity is one of the properties influenced sensitively

Table 7. Parameters and standard deviations for the kinematic viscosities calculated using the Goletz and Tassion equation

	MIPK	[$P_{666,14}$][Cl]	[$P_{666,14}$][DCA]	[$P_{666,14}$][TMPP]
A	0.0411	1.3676	1.5329	3.2897
B	774.24	669.69	495.77	426.89
C	−0.0230	−205.65	−204.61	−216.11
σ_{st}	0.0048	34.7260	8.6415	17.52281

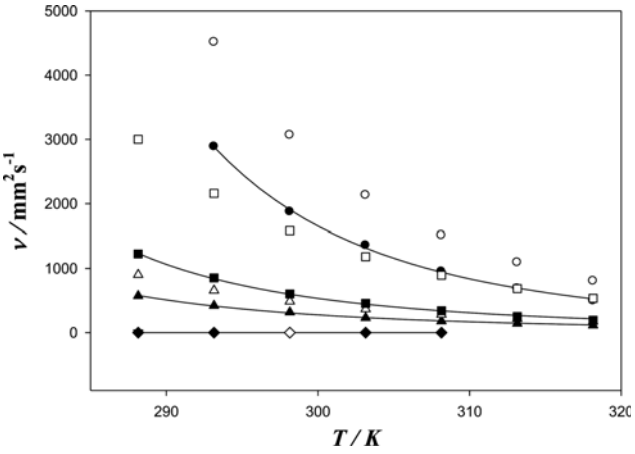

Fig. 3. Kinematic viscosity vs temperature at p=0.1 MPa. ▼, MEK; ◆, MIPK; ●, [$P_{666,14}$][Cl]; ▲, [$P_{666,14}$][DCA]; ■, [$P_{666,14}$][TMPP]; ◇, MIPK was reported by Fermeglia et al. [23]; ○, [$P_{666,14}$][Cl]; △, [$P_{666,14}$][DCA]; □, [$P_{666,14}$][TMPP] were reported by Neves et al. [21]. Solid lines were calculated using the Goletz and Tassion equation.

Table 8. Densities, excess molar volumes, refractive indices and deviations in the molar refractivity for the binary systems at T= 298.15 K and p=0.1 MPa

x_1	ρ/g·cm^{-3a}	V^E/cm^3·mol^{-1}	$n_D{}^b$	ΔR/cm^3·mol^{-1}
{MEK (1)+[$P_{666,14}$][Cl] (2)}				
0.0471	0.8891	−0.2013	1.4808	−7.5753
0.0996	0.8886	−0.3765	1.4790	−16.1385
0.1980	0.8871	−0.5234	1.4769	−31.0644
0.2994	0.8854	−0.7408	1.4759	−45.2124
0.3986	0.8833	−0.9394	1.4729	−58.2200
0.4996	0.8803	−1.0712	1.4690	−69.6590
0.5997	0.8761	−1.1576	1.4643	−78.2833
0.6991	0.8700	−1.1493	1.4564	−82.7376
0.7992	0.8601	−1.0439	1.4474	−79.2442
0.9001	0.8420	−0.7763	1.4237	−60.4862
0.9500	0.8263	−0.5167	1.4062	−38.7515
{MEK (1)+[$P_{666,14}$][DCA] (2)}				
0.0488	0.8994	−0.1390	1.4821	−8.2052
0.1000	0.8989	−0.3493	1.4807	−16.9914
0.1993	0.8974	−0.5942	1.4793	−32.9189
0.2996	0.8956	−0.8386	1.4770	−48.2744
0.4001	0.8932	−1.0260	1.4744	−62.3243
0.4996	0.8899	−1.1214	1.4690	−74.8491
0.5996	0.8852	−1.1556	1.4635	−84.3583
0.7000	0.8784	−1.1629	1.4566	−89.2662
0.8000	0.8676	−1.0775	1.4465	−85.9975
0.9000	0.8475	−0.7926	1.4269	−65.9434
0.9501	0.8293	−0.4499	1.4111	−42.3165
{MEK (1)+[$P_{666,14}$][TMPP] (2)}				
0.0507	0.8852	−0.3312	1.4709	−13.3265
0.1000	0.8850	−0.5598	1.4705	−26.1064
0.1995	0.8842	−0.8290	1.4693	−51.2958
0.3003	0.8829	−0.8629	1.4673	−75.9523
0.4007	0.8811	−0.7826	1.4650	−98.9193
0.4997	0.8786	−0.7001	1.4629	−119.2755
0.6002	0.8752	−0.6221	1.4591	−136.7685
0.6997	0.8702	−0.5310	1.4534	−148.4379
0.7999	0.8619	−0.4436	1.4433	−149.1049
0.9000	0.8456	−0.2884	1.4307	−122.2532
0.9500	0.8297	−0.1549	1.4187	−83.6260
{MIPK (1)+[$P_{666,14}$][Cl] (2)},				
0.0502	0.8888	−0.1518	1.4807	−7.4866
0.1002	0.8881	−0.2934	1.4798	−14.7956
0.1995	0.8864	−0.4973	1.4777	−28.6842
0.2994	0.8841	−0.6306	1.4746	−41.8327
0.4005	0.8812	−0.7393	1.4720	−53.5248
0.5005	0.8774	−0.8057	1.4677	−63.4282
0.6003	0.8724	−0.8803	1.4622	−70.5571
0.7001	0.8653	−0.8956	1.4545	−73.4215
0.8000	0.8545	−0.8393	1.4426	−69.0978
0.8999	0.8363	−0.6264	1.4263	−50.5309
0.9500	0.8216	−0.4302	1.4099	−31.5290

Table 8. Continued

x_1	ρ/g·cm^{-3}[a]	V^E/cm^3·mol^{-1}	n_D[b]	ΔR/cm^3·mol^{-1}
{MIPK (1)+[$P_{666,14}$][DCA] (2)}				
0.0507	0.8992	−0.1696	1.4818	−8.0374
0.0987	0.8985	−0.2958	1.4810	−15.4911
0.2006	0.8965	−0.4967	1.4790	−30.7625
0.3007	0.8943	−0.7893	1.4766	−44.7990
0.3990	0.8915	−0.9993	1.4738	−57.2317
0.5000	0.8876	−1.1430	1.4697	−68.1208
0.5998	0.8823	−1.2542	1.4644	−76.0364
0.7000	0.8747	−1.2696	1.4570	−79.4526
0.7996	0.8631	−1.1964	1.4485	−74.8269
0.9001	0.8430	−0.9556	1.4280	−55.5283
0.9499	0.8261	−0.6497	1.4112	−34.9680
{MIPK (1)+[$P_{666,14}$][TMPP] (2)}				
0.0486	0.8849	−0.1188	1.4706	−12.2800
0.0989	0.8844	−0.2229	1.4698	−24.8040
0.1986	0.8831	−0.2885	1.4687	−48.6476
0.3005	0.8814	−0.3251	1.4673	−71.8645
0.3995	0.8794	−0.3675	1.4650	−93.0135
0.5001	0.8767	−0.4007	1.4625	−112.0210
0.5990	0.8728	−0.4146	1.4586	−127.3123
0.7000	0.8670	−0.3897	1.4524	−136.8910
0.7991	0.8579	−0.3273	1.4425	−135.1162
0.8998	0.8408	−0.2105	1.4269	−107.4412
0.9499	0.8255	−0.1386	1.4134	−71.4743

[a]Standard uncertainties u are u(x)=0.0001, u(ρ)=6×10^{-5} g·cm^{-3}, u(T)=0.01 K

[b]Standard uncertainties u are u(n_D)=1.5×10^{-4}, u(T)=0.05 K

by the presence of water and other impurities. Therefore, large discrepancies of reported viscosities were often observed by different authors. However, as mentioned, we did not consider impurity for the viscosity measurement and for comparing with the reported data.

2. Excess and Deviation Properties

As mixture properties, the measured density and refractive indices for the binary systems of {MEK+[$P_{666,14}$][Cl]}, {MEK+[$P_{666,14}$][DCA]}, {MEK+[$P_{666,14}$][TMPP]}, {MIPK+[$P_{666,14}$][Cl]}, {MIPK+[$P_{666,14}$][DCA]} and {MIPK+[$P_{666,14}$][TMPP]} are listed in Table 8 along with the excess molar volume (V^E) and the deviation of the refractive indices (ΔR) for a temperature of 298.15 K. The V^E for the binary mixtures was determined from the measured densities using Eq. (7) [30,31]

$$V^E/\mathrm{cm}^3\cdot\mathrm{mol}^{-1}=\frac{\Sigma_i x_i M_i}{\rho_m}-\sum_i\left[\frac{x_i M_i}{\rho_i}\right] \tag{7}$$

where x_i, M_i and ρ_i represent the mole fraction, the molar mass and the density of the pure component i, respectively. ρ_m is a density of the mixture.

The ΔR values were calculated from the molar refractivity (R_m) of the pure and mixture components, which were determined from the measured densities and refractive indices using Eqs. (8)-(11) [32,33]:

$$\Delta R/\mathrm{cm}^3\cdot\mathrm{mol}^{-1}=R_m-\Sigma_i\phi_i R_i \tag{8}$$

$$R_m=\left[\frac{n_D^2-1}{n_D^2+1}\right]\left[\frac{\Sigma_i x_i M_i}{\rho_m}\right] \tag{9}$$

$$R_i=\left[\frac{n_{D,i}^2-1}{n_{D,i}^2+1}\right]\left[\frac{M_i}{\rho_i}\right] \tag{10}$$

$$\phi_i=\frac{x_i V_i}{\Sigma_j x_j V_j} \tag{11}$$

where ϕ_i, n_D, $n_{D,i}$ and V_i represent the volume fraction of the pure component i in the mixture, the refractive index of the mixture and the pure component i and the molar volume of the pure component i, respectively.

The binary V^E and ΔR data were correlated with the Redlich-Kister polynomial [4].

$$V^E \text{ or } \Delta R/\mathrm{cm}^3\cdot\mathrm{mol}^{-1}=x_1x_2\Sigma_{i=1}^{n}A_i(x_1-x_2)^{i-1} \tag{12}$$

where x, A_i and n mean mole fraction, regressed equation parameter and number of parameters, respectively. The optimal numbers of parameter were determined by using an Akaike Information

Table 9. The Redlich-Kister parameters and standard deviations for V^E and ΔR for the binary systems at T=298.15 K and p=0.1 MPa

	Systems	A_1	A_2	A_3	A_4	A_5	A_6	σ_{st}/cm^3·mol^{-1}
V^E	{MEK+[$P_{666,14}$][Cl]}	−4.3481	−2.2156	0.1288	−1.2017	−5.1590	-	0.0170
	{MEK+[$P_{666,14}$][DCA]}	−4.4696	−1.4766	−1.7722	−2.6296	−1.2134	-	0.0202
	{MEK+[$P_{666,14}$][TMPP]}	−2.7874	1.7822	−3.5677	1.0000	0.8715	−1.0887	0.0086
	{MIPK+[$P_{666,14}$][Cl]}	−3.2689	−1.5836	−1.9534	0.7143	−1.6383	−3.1842	0.0128
	{MIPK+[$P_{666,14}$][DCA]}	−4.6677	−2.3158	0.0512	−3.7122	−5.7401	-	0.0217
	{MIPK+[$P_{666,14}$][TMPP]}	−1.6059	−0.6248	−0.4315	1.7683	−1.2542	−1.2775	0.0078
ΔR	{MEK+[$P_{666,14}$][Cl]}	−279.4421	−207.8645	−126.9742	−59.7398	−162.6560	−153.3958	0.2597
	{MEK+[$P_{666,14}$][DCA]}	−300.0284	−227.5992	−136.5303	−73.5256	−182.3548	−163.5705	0.2582
	{MEK+[$P_{666,14}$][TMPP]}	−480.2938	−395.5918	−234.1394	−142.4409	−496.1808	−460.2605	1.1887
	{MIPK+[$P_{666,14}$][Cl]}	−253.8944	−175.0312	−110.1286	−68.6205	−96.5991	−74.6462	0.1917
	{MIPK+[$P_{666,14}$][DCA]}	−273.1405	−193.5267	−114.5520	−61.4328	−123.6361	−108.7164	0.2283
	{MIPK+[$P_{666,14}$][TMPP]}	−450.0104	−356.2637	−217.9528	−134.4670	−370.6429	−326.1993	0.7678

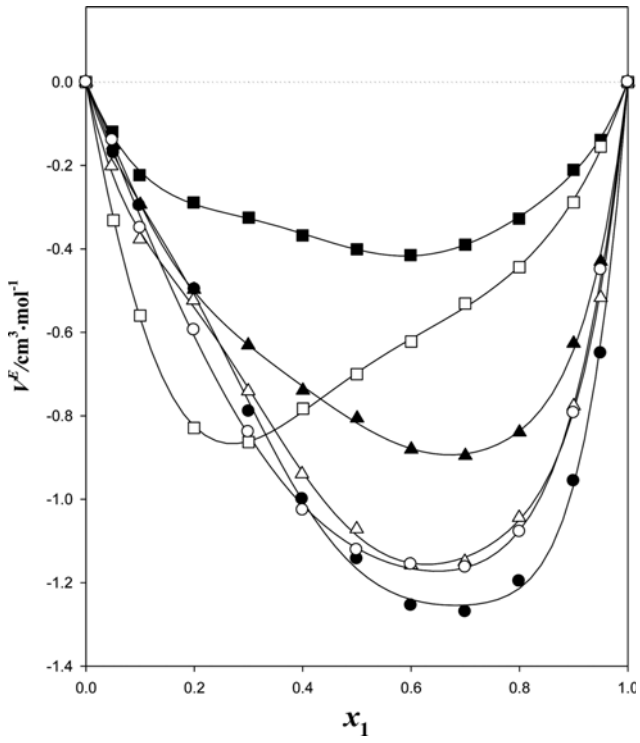

Fig. 4. V^E/(cm^3·mol^{-1}) for the binary systems at 298.15 K. △, {MEK+[$P_{666,14}$][Cl]}; ○, {MEK+[$P_{666,14}$][DCA]}; □, {MEK+[$P_{666,14}$][TMPP]}; ▲, {MIPK+[$P_{666,14}$][Cl]}; ●, {MIPK+[$P_{666,14}$][DCA]}; ■, {MIPK+[$P_{666,14}$][TMPP]}. Solid curves were calculated using the Redlich-Kister parameters.

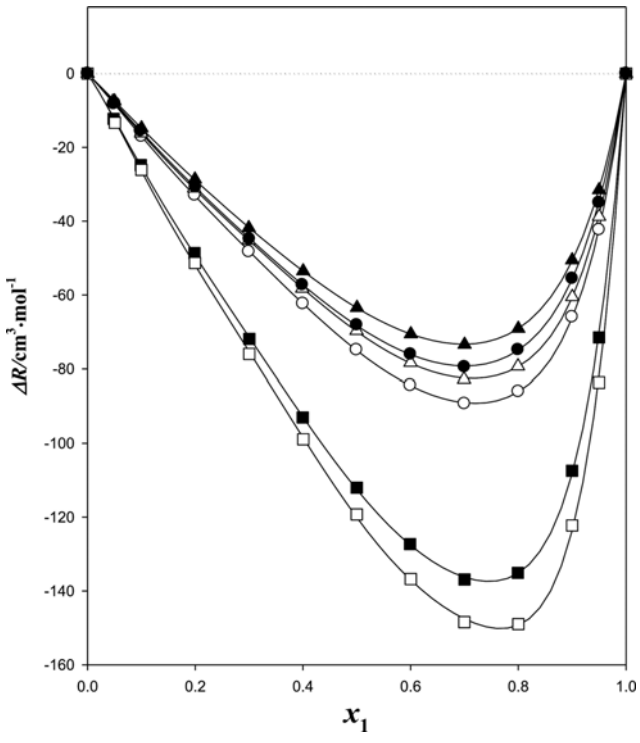

Fig. 5. ΔR/(cm^3·mol^{-1}) for the binary systems at 298.15 K. △, {MEK+[$P_{666,14}$][Cl]}; ○, {MEK+[$P_{666,14}$][DCA]}; □, {MEK+[$P_{666,14}$][TMPP]}; ▲, {MIPK+[$P_{666,14}$][Cl]}; ●, {MIPK+[$P_{666,14}$][DCA]}; ■, {MIPK+[$P_{666,14}$][TMPP]}. Solid curves were calculated using the Redlich-Kister parameters.

Criterion (AIC) [34], which is as follows:

$$AIC = N \ln SSR + 2n \quad (13)$$

where N, SSR and n mean number of data, sum of squares of residuals and number of parameters, respectively. We did not consider more than seven parameters for convenient application to engineering and decided the number of parameters, producing the smallest value for AIC test [35].

The correlated parameters for the experimented binary V^E and ΔR data are listed in Table 9 with their corresponding standard deviations. The constant lines, calculated with the correlated parameters, are in good agreement with the experimental each binary data, as shown in Figs. 4 and 5. The mean deviations of the V^E values between the experimental and calculated data are 0.0170, 0.0202, 0.0086, 0.0128, 0.0217 and 0.0078 cm^3·mol^{-1} for systems {MEK+[$P_{666,14}$][Cl]}, {MEK+[$P_{666,14}$][DCA]}, {MEK+[$P_{666,14}$][TMPP]}, {MIPK+[$P_{666,14}$][Cl]}, {MIPK+[$P_{666,14}$][DCA]} and {MIPK+[$P_{666,14}$][TMPP]}, respectively. The V^E values for all of the binary systems showed negative deviations from ideal behavior, as illustrated in Fig. 4. These deviations may be mainly due to the strong polarity of the amides and chlorides of the ionic liquids and ketones. Hydrogen bonding could also be responsible for the negative deviations from ideality. And the free volume effect due to the difference in structure between ketone and ionic liquid may also have contributed some parts to a negative V^E values [36].

The ΔR of all of the determined binary systems at 298.15 K

Table 10. Absolute average deviation (Δ_{ADD}%) in the calculations of the refractive indices and densities using the different equations: Lorentz-Lorenz (L-L), Gladstone-Dale (G-D), Weiner (W), Heller (H) at 298.15 K

Binary systems	n_D, Δ_{ADD}%				ρ, Δ_{ADD}%
	L-L	G-D	W	H	L-L
{MEK+[$P_{666,14}$][Cl]}	0.1450	0.1190	0.1292	0.1752	0.1230
{MEK+[$P_{666,14}$][DCA]}	0.1362	0.1084	0.1194	0.1819	0.2082
{MEK+[$P_{666,14}$][TMPP]}	0.1112	0.0958	0.0998	0.1532	0.2903
{MIPK+[$P_{666,14}$][Cl]}	0.1016	0.0770	0.0865	0.1348	0.0895
{MIPK+[$P_{666,14}$][DCA]}	0.1502	0.1254	0.1350	0.1848	0.0901
{MIPK+[$P_{666,14}$][TMPP]}	0.0378	0.0278	0.0316	0.0628	0.0714

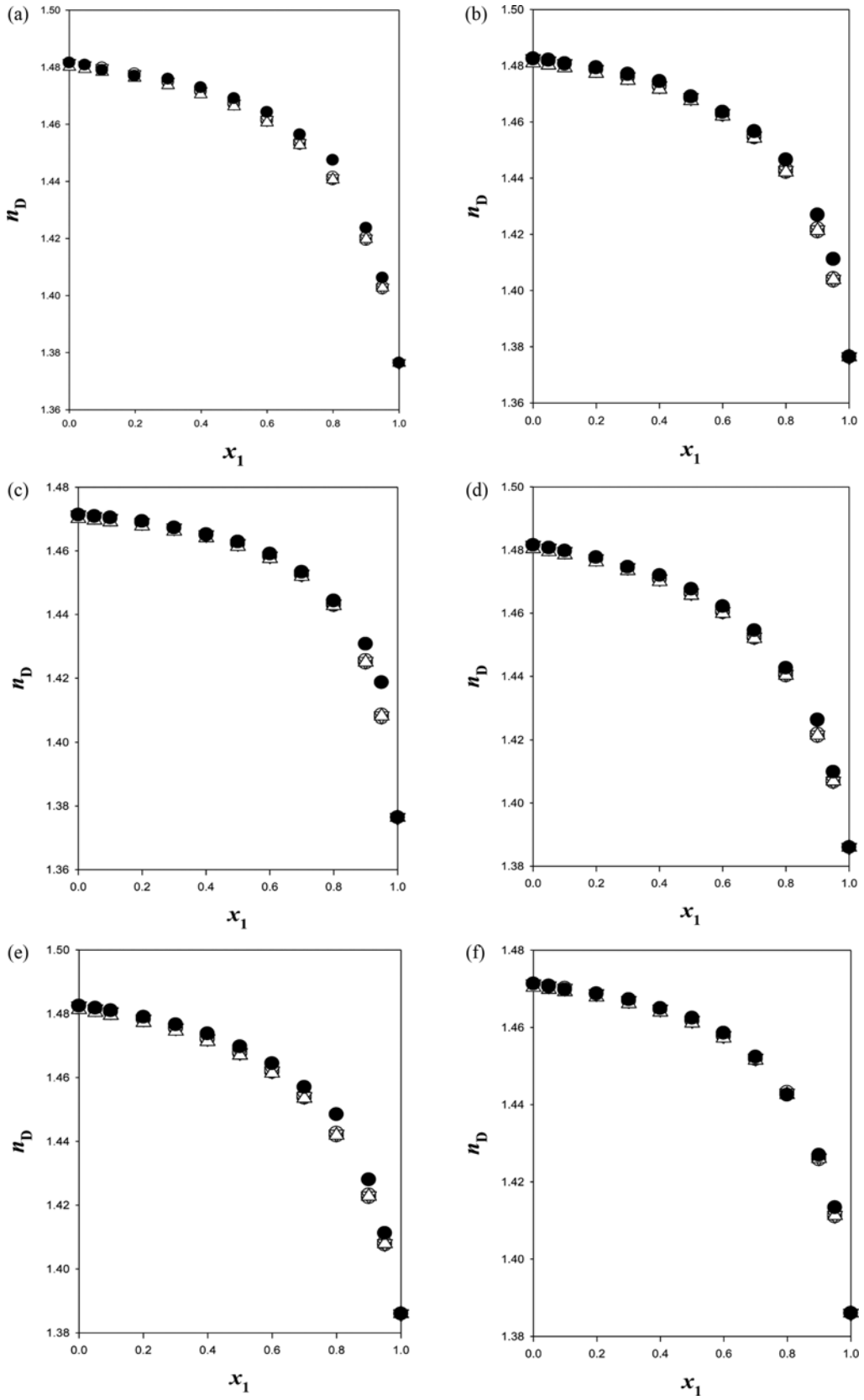

Fig. 6. Refractive indices, n_D, for the binary system at 298.15 K. (a) {MEK+[$P_{666.14}$][Cl]}, (b) {MEK+[$P_{666.14}$][DCA]}, (c) {MEK+[$P_{666.14}$][TMPP]}, (d) {MIPK+[$P_{666.14}$][Cl]}, (e) {MIPK+[$P_{666.14}$][DCA]}, (f) {MIPK+[$P_{666.1}$4][TMPP]}. ●, Experimental data; ○, data calculated using the L-L equation; △, data calculated using the Gladstone-Dale equation; □, data calculated using the Weiner equation; ◇, data calculated using the Gladstone-Dale equation.

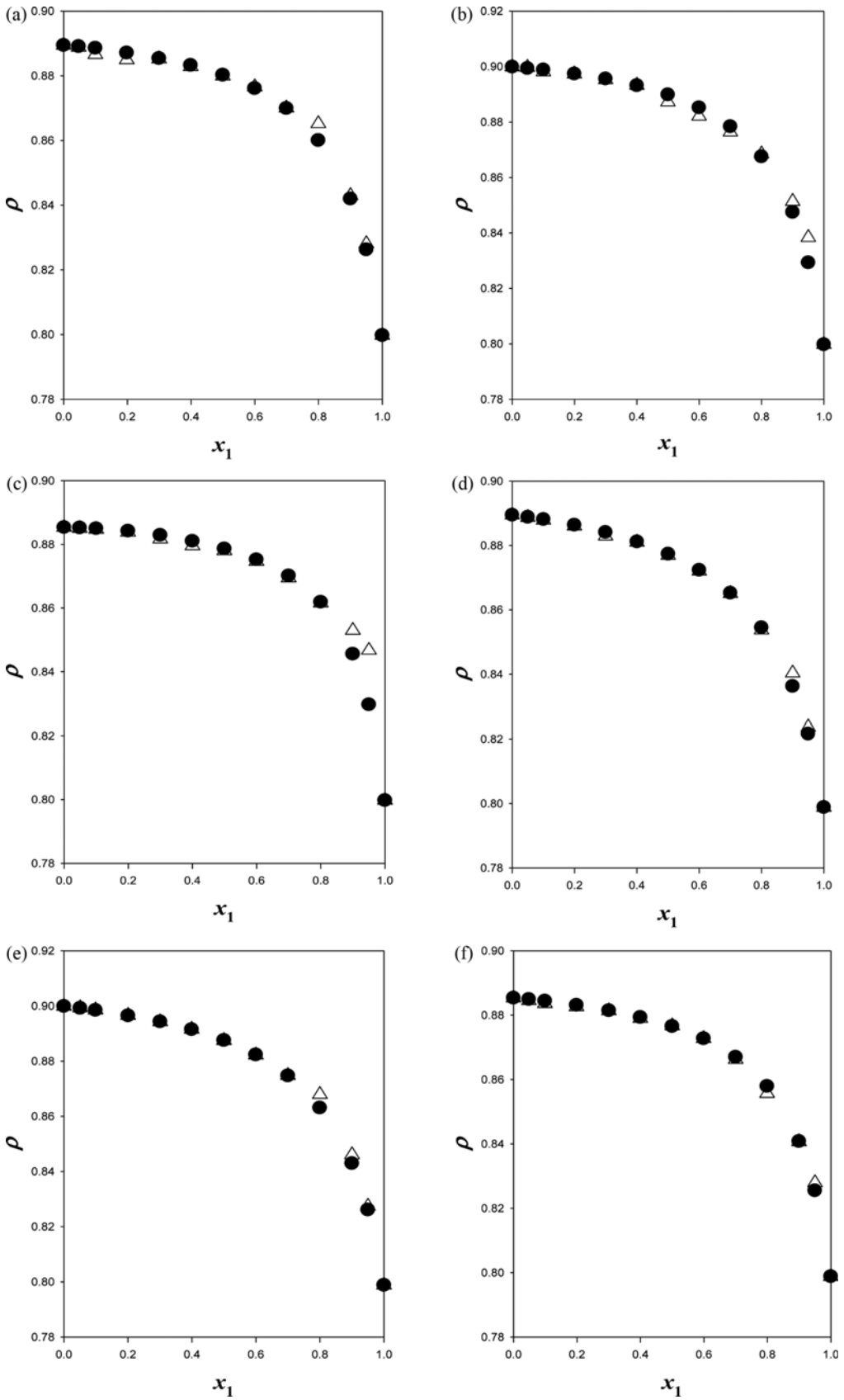

Fig. 7. Densities, ρ/g·cm^{-3}, for the binary system at 298.15 K. (a) {MEK+[$P_{666.14}$][Cl]}, (b) {MEK+[$P_{666.14}$][DCA]}, (c) {MEK+[$P_{666.14}$][TMPP]}, (d) {MIPK+[$P_{666.14}$][Cl]}, (e) {MIPK+[$P_{666.14}$][DCA]}, (f) {MIPK+[$P_{666.1}$4][TMPP]}. ●, Experimental data; △, data calculated using the Lorentz-Lorenz refractive index mixing rule.

showed relatively large negative values over the entire composition range, as illustrated in Fig. 5. These large negative values may be due to the large differences in size between the ionic liquids and the ketone-type compounds. The magnitude of the negativity was ordered for the system as follows: {MEK+[$P_{666,14}$][TMPP]}>{MIPK+[$P_{666,14}$][TMPP]}>{MEK+[$P_{666,14}$][DCA]}>{MEK+[$P_{666,14}$][Cl]}>{MIPK+[$P_{666,14}$][DCA]}>{MIPK+[$P_{666,14}$][Cl]}. This order is consistent with the order of the size of the molar volumes of the phosponium-based ionic liquids. The refractive index of the mixture strongly depends on the liquid structure and the molecular interactions [37]. Therefore, ΔR showed different deviation phenomenon compared with the V^E values for the same systems. In general, the negative deviations in ΔR were due to the presence of the significant interactions between the mixture components [38,39]. According to the Redlich-Kister correlation, the mean deviations of ΔR were 0.2597, 0.2582, 1.1887, 0.1917, 0.2283 and 0.7678 $cm^3 \cdot mol^{-1}$ for the binary systems {MEK+[$P_{666,14}$][Cl]}, {MEK+[$P_{666,14}$][DCA]}, {MEK+[$P_{666,14}$][TMPP]}, {MIPK+[$P_{666,14}$][Cl]}, {MIPK+[$P_{666,14}$][DCA]} and {MIPK+[$P_{666,14}$][TMPP]}, respectively.

3. Predictions of Refractive Indices and the Densities for the Binary Systems

The experimental refractive indices and densities and were compared with the predicted values from some model equations. The refractive indices of the aforementioned same binary systems were predicted using the mixing rules proposed by Lorentz-Lorenz [5], Gladstone-Dale [6], Weiner [7], and Heller [8], corresponding with Eqs. (14)-(17), respectively:

$$\frac{n_D^2-1}{n_D^2+2}=\Sigma_{i=1}^{2}\phi_i\left[\frac{n_{D,i}^2-1}{n_{D,i}^2+2}\right] \tag{14}$$

$$n_D-1=\Sigma_{i=1}^{2}\phi_i(n_{D,i}-1) \tag{15}$$

$$\frac{n_D^2-n_{D,1}^2}{n_D^2+2n_{D,1}^2}=\phi_2\left[\frac{n_{D,2}^2-n_{D,1}^2}{n_{D,2}^2+2n_{D,1}^2}\right] \tag{16}$$

$$\frac{n_D-n_{D,1}}{n_{D,1}}=\frac{3}{2}\phi_2\left[\frac{\left(\frac{n_{D,2}}{n_{D,1}}\right)^2-1}{\left(\frac{n_{D,2}}{n_{D,1}}\right)^2+2}\right] \tag{17}$$

In these equations, n_D, $n_{D,i}$ and ϕ_i are the refractive indices of the mixture, the pure component i and the volume fraction of the component i, respectively.

The predictions of the refractive indices are based on the theories of mixing. The deviations from the experimental data were calculated as the absolute average deviation (Δ_{ADD}%) the following, Eq. (18):

$$\Delta_{ADD}\%=\left(\frac{100}{N}\right)\Sigma_{i=1}^{N}\left|\frac{X_i^{exp}-X_i^{calc}}{X_i^{exp}}\right| \tag{18}$$

where X_i^{exp} is the experimental value of the property and X_i^{calc} is the calculated value. The results of the predictions are given in Table 10 and are represented in Fig. 6. As illustrated in the figure, the predicted values showed a little smaller value than experimental values in entire concentration regions. However, Δ_{ADD}% was less than 0.2 for all binary systems.

In the case of binary mixtures density, they were estimated using the expression proposed by Nakata and Sakurai [2,40], in which the mixing rules for the refractive indices are expressed as functions of the volume fractions of the mixture. We used the Lorentz-Lorenz refractive index mixing rule, and then obtained predictions of the densities of the binary mixtures from the following, Eq. (19):

$$\frac{\Sigma_i x_i M_i}{\rho}-\sum_i\frac{x_i M_i}{\rho_i} =-\left[\frac{6n_D}{(n_D^2-1)(n_D^2+2)}\right]\left[\sum_i\left(\frac{x_i M_i}{\rho_i}\right)\right][n_D-(n_{D,1}\phi_1+n_{D,2}\phi_2)] \tag{19}$$

where ρ and n_D are the density and refractive index for the binary mixture, respectively, $n_{D,1}$ and $n_{D,2}$ are the refractive index of pure components 1 and 2, respectively, ϕ_1 and ϕ_2 are the volume fractions of pure components 1 and 2, respectively, and M_i, ρ_i and x_i are the molar mass, density and molar fraction of the pure component i. The predicted densities of the binary mixtures were compared with the experimentally measured values in Fig. 7, and the results are also reported in terms of the percentage of the absolute average deviation in Table 10 [2]. As illustrated in the figures, the predicted values usually showed a little larger values than experimental values in ketone-rich regions, especially for MEK containing mixtures. However, the absolute average deviation according to Eq. (18) was at least less than 0.3%.

CONCLUSIONS

The temperature dependency of pure densities, refractive indices and kinetic viscosities of some possible Mo solvents--MIPK, MEK, [$P_{666,14}$][Cl], [$P_{666,14}$][DCA] and [$P_{666,14}$][TMPP]--were determined. The determined pure properties decreased with increasing temperature. However, viscosity of MIPK has no significant temperature dependency in the measured temperature ranges. The determined physical properties correlated well with the DIPPR, linear, and Goletz and Tassion equations within ca. 1% deviation. They were also compared with the available reported data, and agreed well for density and refractive indices, while the viscosities for ionic liquids showed large discrepancies.

The predictions of the refractive index values were made by using various equations. Some of them, the Gladstone-Dale equation showed the most closed values within 0.2% average deviation. Meanwhile, density data correlated well with the Lorentz-Lorenz refractive index mixing rule within less than 0.3% of average deviation.

The determined V^E and ΔR data for the binary systems showed negative deviations from the ideal behavior due to the strong polarity of the constituents and their differences in molecular size. The V^E and ΔR data correlated well with the Redlich-Kister equation.

ACKNOWLEDGEMENTS

This work was supported by research fund of Chungnam National University.

REFERENCES

1. Molybdenum, Chemicool Periodic Table. Chemicool.com. 17. Oct.

2012. http://www.chemicool.com/elements/molybdenum.html.
2. A. M. Faneite, S. I. Garcés, J. A. Aular, M. R. Urdaneta and D. Soto, *Fluid Phase Equilib.*, **334**, 117 (2012).
3. A. N. Soriano, B. T. Doma and M. H. Li, *J. Taiwan Inst. Chem. Eng.*, **41**, 115 (2010).
4. O. Redlich and A. T. Kister, *Ind. Eng. Chem.*, **40**, 345 (1948).
5. H. A. Lorentz, *Wied. Ann. Phys.*, **9**, 641 (1880).
6. T. P. Dale and J. H. Gladstone, *Phil. Trans. R. Soc. Lond.*, **148**, 887 (1858).
7. O. Wiener, *Berichte über die Verhandlungen der Königlich-Sächsischen Gesellschaft der Wisseschaften zu Leipzig*, **62**, 256 (1910).
8. W. Heller, *J. Phys. Chem.*, **69**, 1123 (1965).
9. S. Faranda, G. Foca, A. Marchetti, G. Pályi, L. Tassi and C. Zucchi, *J. Mol. Liq.*, **111**, 117 (2004).
10. J. Wisniak, *Thermochim. Acta*, **257**, 51 (1995).
11. S. Psutka and I. Wichterle, *Fluid Phase Equilib.*, **264**, 55 (2008).
12. I.-C. Hwang, S.-J. Park and K.-J Han, *Fluid Phase Equilib.*, **309**, 145 (2011).
13. F. A. Gonçalves, C. S. Costa, C. E. Ferreira, J. C. Bernardo, I. Johnson, I. M. Fonseca and A. G. Ferreira, *J. Chem. Thermodyn.*, **43**, 914 (2011).
14. I.-Y. Jeong, R.-H. Kwon, S.-J. Park and Y.-Y. Choi, *J. Chem. Eng. Data*, **59**, 289 (2014).
15. J. M. Resa, C. González and J. M. Goenaga, *J. Chem. Eng. Data*, **51**, 73 (2006).
16. A. P. Fröba, H. Kremer and A. Leipertz, *J. Phys. Chem. B*, **112**, 12420 (2008).
17. A. Laesecke, T. J. Fortin and J. D. Splett, *Energy Fuels*, **26**, 1844 (2012).
18. T. J. Fortin, A. Laesecke, M. Freund and S. Outcalt, *J. Chem. Thermodyn.*, **57**, 276 (2013).
19. R. D. Chirico, M. Frenkel, J. W. Magee, V. Diky, C. D. Muzny, A. F. Kazakov, K. Kroenlein, I. Abdulagatov, G. R. Hardin, W. E. Acree, J. F. Brenneke, P. L. Brown, P. T. Cummings, T. W. de Loos, D. G. Friend, A. R. Goodwin, L. D. Hansen, W. M. Haynes, N. Koga, A. Mandelis, K. N. Marsh, P. W. Mathias, C. McCabe, J. P. O'Connell, A. Padua, V. Rives, C. Schick, J. P. Trusler, S. Vyazovkin, R. D. Weier and J. Wu, *J. Chem. Eng. Data*, **58**, 2699 (2013).
20. J. A. Widegren, A. Laesecke and J. W. Magee, *Chem. Commun.*, **12**, 1610 (2005).
21. C. M. Neves, P. J. Carvalho, M. G. Freire and J. A. Coutinho, *J. Chem. Thermodyn.*, **43**, 948 (2011).
22. J. C. Rintelen, J. H. Saylor and P. M. Gross, *J. Am. Chem. Soc.*, **59**, 1129 (1937).
23. M. Fermeglia, R. Lapasin and G. Torriano, *J. Chem. Eng. Data*, **35**, 260 (1990).
24. R. A. Clará, A. G. Marigliano and H. N. Sólimo, *J. Chem. Eng. Data*, **51**, 1473 (2006).
25. T. W. Mears, A. Fookson, P. Pomerantz, E. H. Rich, C. S. Dussinger and F. L. Howard, *J. Res. Natl. Bur. Stand.*, **44**, 299 (1950).
26. H. F. Almeida, J. A. Lopes-da-Silva, M. G. Freire and J. A. Coutinho, *J. Chem. Thermodyn.*, **57**, 372 (2013).
27. L. D. Lorenzi, M. Fermeglia and G. Torriano, *J. Chem. Eng. Data*, **43**, 183 (1998).
28. T. E. Daubert and R. P. Danner, *Physical and Thermodynamic Properties of Pure Chemicals*, Hemisphere Publishing Corp., New York (1989).
29. R. C. Reid, J. M. Prausnitz and B. E. Poling, *The Properties of Gases and Liquids*, 4th Ed., McGraw-Hill, Singapore (1989).
30. J.-H. Oh and S.-J. Park, *J. Chem. Eng. Data*, **43**, 1009 (1998).
31. K.-J. Han, J.-H. Oh, S.-J. Park and J. Gmehling, *J. Chem. Eng. Data*, **50**, 1951 (2005).
32. T. M. Aminabhavi and B. Gopalakrishna, *J. Chem. Eng. Data*, **40**, 856 (1995).
33. A. H. Al-Dujaili, A. A. Yassen and A. M. Awwad, *J. Chem. Eng. Data*, **45**, 647 (2000).
34. H. Akaike, *IEEE T. Automat. Contr.*, **19**, 716 (1974).
35. L. Kirkup, *Data Analysis with Excel*, Cambridge University Press: Cambridge (2002).
36. J.-I. Kim, S.-J. Park, S.-B. Kim and Y.-Y. Choi, *Fluid Phase Equilib.*, **314**, 7 (2012).
37. W. Kauzman and H. Eyring, *J. Am. Chem. Soc.*, **62**, 3113 (1940).
38. P. Brocos, A. Pineiro, R. Bravo and A. Amigo, *Phys. Chem. Chem. Phys.*, **5**, 550 (2003).
39. A. K. Nain, *J. Chem. Eng. Data*, **53**, 850 (2008).
40. M. Nakata and M. Sakurai, *J. Chem. Soc. Faraday Trans.*, **83**, 2449 (1987).